

GALACTIC MICROWAVE EMISSION AT DEGREE ANGULAR SCALES

Angélica de Oliveira-Costa^{1,2}

A. Kogut³

Mark J. Devlin⁴

C. Barth Netterfield⁵

Lyman A. Page¹

Edward J. Wollack⁶

¹Princeton University, Department of Physics, Jadwin Hall, Princeton, NJ 08544;
angelica@tatania.princeton.edu

²Institute for Advanced Study, Olden Lane, Princeton, NJ 08540

³Hughes STX Corporation, Laboratory for Astronomy and Solar Physics, Code 685,
NASA/GSFC, Greenbelt, MD 20771

⁴University of Pennsylvania, Department of Physics and Astronomy, David Rittenhouse
Laboratory, Philadelphia, PA 19104

⁵California Institute of Technology, MS 59-33, Pasadena, CA 91125

⁶National Radio Astronomy Observatory, Central Development Laboratory, 2015 Ivy Road,
Charlottesville, VA 22903

Received _____; accepted _____

ApJ Lett, 482:L17-20 (1997)

ABSTRACT

We cross-correlate the Saskatoon Ka and Q-Band Cosmic Microwave Background (CMB) data with different maps to quantify possible foreground contamination. We detect a marginal correlation ($\gtrsim 2\sigma$) with the Diffuse Infrared Background Experiment (DIRBE) 240, 140 and 100 μm maps, but we find no significant correlation with point sources, with the Haslam 408 MHz map or with the Reich and Reich 1420 MHz map. The *rms* amplitude of the component correlated with DIRBE is about 20% of the CMB signal. Interpreting this component as free-free emission, this normalization agrees with that of Kogut et al. (1996a; 1996b) and supports the hypothesis that the spatial correlation between dust and warm ionized gas observed on large angular scales persists to smaller angular scales. Subtracting this contribution from the CMB data reduces the normalization of the Saskatoon power spectrum by only a few percent.

Subject headings: methods: data analysis – cosmic microwave background

1. INTRODUCTION

One of the major concerns in any Cosmic Microwave Background (CMB) anisotropy analysis is to determine if the observed signal is due to real CMB fluctuations or due to some foreground contaminant. At the frequency range and angular scale of the Saskatoon experiment (Wollack et al. 1997, hereafter W97; Netterfield et al. 1997, hereafter N97), there are two major potential sources of foreground contamination: diffuse Galactic emission and unresolved point sources.

The diffuse Galactic contamination includes three components: synchrotron and free-free radiation, which are important mainly at frequencies below 60 GHz, and thermal emission from dust particles, which is important mainly at frequencies above 60 GHz (see, e.g., Partridge 1995; Bennett et al. 1992, Brandt et al. 1994, Bennett et al. 1996). From the theoretical point of view, it is possible to distinguish these three components by observing their different frequency dependence and spatial morphology. In practice, however, there is no emission component for which both the frequency dependence and spatial template are currently well known (see, e.g., Kogut et al. 1996a, hereafter K96a, and references therein).

Upper limits have been placed on the different contaminants at the frequency range and angular scale of the Saskatoon experiment. For instance, by extrapolating radio maps at 408 MHz (Haslam et al. 1981) and 1420 MHz (Reich and Reich 1988) to 40 GHz, N97 place an upper limit on *rms* fluctuations in the synchrotron emission of $3 \mu\text{K}$ within the Saskatoon observing region. From analysis done on $\text{H}\alpha$ maps of the Saskatoon observing region, Gaustad et al. (1996) and Simonetti et al. (1996) place an upper limit on *rms* fluctuations in the diffuse free-free emission of $2 \mu\text{K}$ at 40 GHz. An analysis of the Galactic emission in the Differential Microwave Radiometer (DMR) map at 53 GHz places limits of $(3.4\pm 3.7) \mu\text{K}$ for the synchrotron emission, $(7.1\pm 1.7) \mu\text{K}$ for the free-free, and $(2.7\pm 1.3) \mu\text{K}$ for the dust emission, for $|b| > 30^\circ$ (Kogut et al. 1996b, hereafter K96b). Extrapolating these DMR results to degree angular scales, Tegmark and Efstathiou (1996) obtained an upper limit of $2 \mu\text{K}$ for dust emission at 40 GHz.

The purpose of this *Letter* is to use the Saskatoon data (W97, N97; Tegmark et al. 1997,

hereafter T97) to estimate the Galactic emission at degree angular scales. In the following sections, we present the technique used to identify the Galactic emission and the results obtained from the cross-correlation of the Saskatoon data with different Galactic templates.

2. THE METHOD

The Saskatoon data set consists of $N=2586$ observed data points y_{SK}^i (not including “ring data”), each containing the true CMB temperature fluctuations in the sky \mathbf{x}_{CMB} convolved with some beam function, and with noise \mathbf{n}_i added afterwards. We assume that the Saskatoon data are a superposition of the CMB fluctuations and Galactic signals whose angular distributions are traced by an external data set (K96a; K96b). Combining these numbers into vectors \mathbf{y}_{SK} , \mathbf{x}_{CMB} and \mathbf{n} , respectively, we can therefore write

$$\mathbf{y}_{SK} = \mathbf{F}\mathbf{x}_{CMB} + \mathbf{n} + \alpha\mathbf{F}\mathbf{x}_{Gal}, \quad (1)$$

where \mathbf{F} is the beam function matrix defined in T97, x_{Gal}^i are the brightness fluctuations of the Galactic template map (not necessarily in temperature units), and α is the coefficient that converts the Galactic template into antenna temperature. Since $\langle \mathbf{x}_{CMB} \rangle = \langle \mathbf{n} \rangle = 0$, and $\mathbf{F}\mathbf{x}_{Gal}$ ($\equiv \mathbf{y}_{Gal}$) is a constant vector, the data covariance matrix is given by

$$\mathbf{C} \equiv \langle \mathbf{y}_{SK}\mathbf{y}_{SK}^T \rangle - \langle \mathbf{y}_{SK} \rangle \langle \mathbf{y}_{SK}^T \rangle = \mathbf{F}\langle \mathbf{x}_{CMB}\mathbf{x}_{CMB}^T \rangle \mathbf{F}^T + \langle \mathbf{n}\mathbf{n}^T \rangle, \quad (2)$$

where $\langle \mathbf{x}_{CMB}\mathbf{x}_{CMB}^T \rangle$ is the correlation between the data points and themselves, and $\langle \mathbf{n}\mathbf{n}^T \rangle$ is the noise covariance matrix. The former is given by the angular power spectrum C_ℓ through the familiar relation

$$\langle x_{CMB}^i x_{CMB}^j \rangle = \sum_{\ell=0}^{\infty} \frac{2\ell+1}{4\pi} P_\ell(\cos \theta_{i,j}) C_\ell, \quad (3)$$

where ℓ is the multipole number, P_ℓ are the Legendre polynomials, and $\theta_{i,j}$ is the angle between pixels i and j .

By minimizing $\chi^2 \equiv (\mathbf{y}_{SK} - \alpha\mathbf{y}_{Gal})^T \mathbf{C}^{-1} (\mathbf{y}_{SK} - \alpha\mathbf{y}_{Gal})$ we can obtain $\hat{\alpha}$, the minimum-variance

estimate of α . From $\frac{\partial \chi^2}{\partial \alpha} \equiv 0$, we find that

$$\hat{\alpha} = \frac{\mathbf{y}_{Gal}^T \mathbf{C}^{-1} \mathbf{y}_{SK}}{\mathbf{y}_{Gal}^T \mathbf{C}^{-1} \mathbf{y}_{Gal}} \quad (4)$$

with variance

$$\sigma_{\hat{\alpha}}^2 = \frac{1}{(\mathbf{y}_{Gal}^T \mathbf{C}^{-1} \mathbf{y}_{Gal})}. \quad (5)$$

This variance accounts for the effect of chance alignments between the CMB and the various template maps, since the CMB anisotropy term is included in equation (3). We compute \mathbf{C} as described in T97, with a flat power spectrum $C_\ell = 6Q^2/\ell(\ell + 1)$ normalized to $Q=47 \mu\text{K}$. Note that our analysis is performed on the Saskatoon scan data \mathbf{y}_{SK} , and not on the Wiener-filtered Saskatoon maps.

3. DATA ANALYSIS AND RESULTS

The analysis is based on the 1993-1995 data from Saskatoon experiment (W97, N97, T97). We treated the Ka-Band data (26 to 36 GHz) separately from the Q-Band data (36-46 GHz) in order to gain additional frequency information on any correlated emission. However, it is important to remember that observations made on Ka-Band constitute less than a quarter of the total data set, and therefore give substantially noisier estimates.

The Saskatoon data are insensitive to the monopole ($\ell=0$), and only marginally sensitive to other low order ℓ . Accordingly, when we convolve the template maps with the Saskatoon beam function, we are removing the mean of the templates, as well as large angular scale structures. As a consequence, our results depend predominantly on the small scale intensity variations in the templates ($\ell>30$) and are insensitive to the zero levels of the Saskatoon data and the template maps.

We cross-correlate the Saskatoon data with two different synchrotron templates: the 408 MHz survey (Haslam et al. 1981) and the 1420 MHz survey (Reich and Reich 1988). To study dust and free-free emission, we cross-correlate the Saskatoon data with three Diffuse Infrared Background

Experiment (DIRBE) sky maps at wavelengths 240, 140 and 100 μm (Boggess et al. 1992). In order to study the extent of point source contamination in the Saskatoon data, we cross-correlate with the 1 Jy catalog of point sources at 5 GHz (Kühr et al. 1981). The templates used in this analysis, as well as the previously described Saskatoon data, are shown in Figure 1.

Tables 1 and 2 show the coefficients $\hat{\alpha}$ and the resulting fluctuations in antenna temperature in the Saskatoon Ka and Q-Band data, $\Delta T = \hat{\alpha} \sigma_{Gal}$, where σ_{Gal} is the standard deviation of the template map,

$$\sigma_{Gal}^2 = \frac{\mathbf{y}_{Gal}^T \mathbf{y}_{Gal}}{N}. \quad (6)$$

The values of σ_{Gal} were obtained directly from the template maps after removing monopole and dipole, and smoothing them by a 1° Gaussian, while σ_{Gal} for the Saskatoon data correspond to the *rms* variance at 1° , defined as

$$\sigma_{SK}^2 = \sum_{\ell=0}^{\infty} \left(\frac{2\ell+1}{4\pi} \right) C_\ell W_\ell^2, \quad (7)$$

where W_ℓ is the Saskatoon beam function as defined in N97. The synchrotron templates, as well as the point source template, are found to be uncorrelated with the Saskatoon data¹. All three DIRBE far-infrared templates show a correlation, indicating a detection of signal with common spatial structure in the two data sets. Since the three DIRBE maps trace the same Galactic contamination component, they provide nearly identical estimates of the Galactic emission. The error bars on the correlation between any of the DIRBE templates and the Saskatoon map are dominated by noise and CMB signal (random alignments) in the Saskatoon map. For definiteness, we use the DIRBE 100 μm channel and the correlations obtained for the Saskatoon Q-Band data when placing limits below, since these are the least noisy channels.

K96 detect a positive correlation between the DIRBE far-infrared maps and the DMR maps at 31.5, 53, and 90 GHz. From the spectral index of the correlation (rising strongly at long wave-

¹ We remind the reader that systematic effects (such as striping) are present in the synchrotron radio maps, and may be partially responsible for the null results of the synchrotron cross-correlations.

lengths) they identify the source as a superposition of dust and free-free emission. The weaker signal and more restricted frequency coverage preclude such an unambiguous identification in the Saskatoon data set. The spectral index (of the emission component correlated with DIRBE) between the Ka and Q-band, $\beta = -0.4 \pm 2.1$, is compatible with an origin from dust emission, free-free emission, or chance alignments. However, the amplitude of the signal is much larger than expected for dust emission², leaving free-free emission and chance alignments as the alternatives. As mentioned, our calculation of $\sigma_{\hat{\alpha}}$ includes the effect of chance alignments between the CMB and the various template maps. Assuming that the hypothesis of K96 can be extended to Saskatoon scales, we argue that the correlation between the DIRBE template and the Saskatoon data is most likely due to free-free contamination. As shown in Table 2, the probability that such a strong correlation is caused by chance alignments is a few percent.

We tested the cross-correlation technique by analyzing 1000 constrained realizations of CMB and Saskatoon instrument noise. We recovered unbiased estimates $\hat{\alpha}$ with a variance in excellent agreement with equation (5). As an additional test, we generated simulated DIRBE patches by replacing our DIRBE region with an equivalent patch selected from somewhere else in the sky. Since the *rms* signal in the DIRBE map depends strongly on latitude, we restricted the patches to lie in the latitude range $20^\circ < |b| < 34^\circ$, corresponding to the latitude range of the Saskatoon observing region. In Figure 2, we plot the cumulative distribution for the correlation $C \equiv \left(\frac{\hat{\alpha}}{\sigma_{Gal}} \right) \sigma_{Gal}^{NCP}$ between Saskatoon Q-Band data and the 288 selected patches of the DIRBE 100 μK map, where σ_{Gal}^{NCP} is the standard deviation of the patch actually observed by Saskatoon. This distribution is seen to agree well with a Gaussian distribution with variance given by equation (5), even though the statistical properties of the DIRBE patches themselves are, of course, not Gaussian. Specifically, 284 of the 288 patches (or 98.6% of them) are less correlated with the the Saskatoon Q-Band data than the correct DIRBE patch, in good agreement with the significance level of 97% computed using a Gaussian distribution. The same tests were carried out for the DIRBE 240 and 140 μm maps

² If the entire Saskatoon-DIRBE correlation is due to dust emission, then DMR should see a larger signal.

and for the Saskatoon Ka-Band data, giving similar results.

Due to the proximity of the Saskatoon observing region to the Galactic plane, one might conjecture that the bulk of the Saskatoon-DIRBE correlation is not due to a small scale physical association of dust and free-free emission, but is caused by large scale gradients common to all three diffuse Galactic foreground components (including synchrotron). However, the data do not support this hypothesis: we cross-correlated the DIRBE 100 μm and Haslam maps of the Saskatoon observing region and found no significant correlation.

In summary, the Saskatoon-DIRBE correlation at 30 and 40 GHz is compatible with the free-free emission detected by DMR at 31.5 GHz, assuming an ℓ^{-3} power spectrum for diffuse free-free emission. The Saskatoon value is slightly larger than upper limits from direct H α images, although the uncertainties are substantial. We note that the inferred H α limits assume an electron temperature $T_e \approx 8000$ K; a lower electron temperature would produce a larger microwave signal for fixed H α intensity. A compilation of free-free limits and detections on various angular scales is given in Table 3.

4. CONCLUSIONS

The cross-correlation technique introduced by K96a and K96b provides a powerful way of measuring the level of Galactic foreground contamination.

The synchrotron templates, as well as the point source template, are uncorrelated with the Saskatoon data. We find a cross-correlation (at 97% confidence) between the Saskatoon Q-Band data and the DIRBE 100 μm map. The *rms* amplitude of the contamination correlated with DIRBE 100 μm is ≈ 17 μK at 40 GHz. We argue that the hypothesis of free-free contamination at degree angular scales is the most likely explanation for this correlated emission. Accordingly, the spatial correlation between dust and warm ionized gas observed on large angular scales seems to persist down to the smaller angular scales.

As reported by N97, the angular power spectrum from the Saskatoon data is $\delta T_\ell = 49_{-5}^{+8}$ μK at

$l=87$ (corresponding to *rms* fluctuations around $90 \mu\text{K}$ on degree scales), which is a much higher signal than any of the contributions from the foreground contaminants discussed above, confirming that the Saskatoon data is not seriously contaminated by foreground sources. Since the foreground and the CMB signals approximately add in quadrature, a foreground signal with 20% of the CMB *rms* causes the CMB fluctuations to be over-estimated by $\sqrt{1 + 0.20^2} - 1 \approx 2\%$.

In the course of this analysis, we became aware that Erik Leitch and collaborators have found a correlation between IRAS $100 \mu\text{m}$ map and Owens Valley data; these results are forthcoming. We would like to thank Norman C. Jarosik, Max Tegmark and David T. Wilkinson for many useful comments on the manuscript. Support for this work was provided by a David & Lucile Packard Foundation Fellowship. AC acknowledges the RAPT Foundation for financial support under process No. 314159(IIH). We acknowledge the NASA office of Space Sciences, the COBE flight team, and all those who helped process and analyze the DIRBE data.

Table 1: Correlations with the Saskatoon (SK) Ka-Band (30 GHz)^(a)

Template	$\hat{\alpha} \pm \sigma_{\hat{\alpha}}^{(b)}$	$\frac{\hat{\alpha}}{\sigma_{\hat{\alpha}}}$	Significance ^(c) (%)	$\sigma_{Gal}^{(d)}$	$\Delta T \equiv \hat{\alpha} \sigma_{Gal}$ (μK)	$\frac{\Delta T}{\sigma_{SK}}^{(e)}$ (%)
SK (Ka-Band)	1.00±0.04	23.4	100	90.9	90.9±3.9	100
DIRBE 100 μm	11.8±10.4	1.1	87	1.30	15.3±13.5	17
Point Sources	4.3±10.7	0.4	66	0.50	2.2±5.3	2
408 MHz survey	−4.3±9.6			1.33	−5.8±12.9	−6
1420 MHz survey	−0.04±0.31			0.03	−0.00±0.01	−0.002

^(a) 30 GHz and 40 GHz are, respectively, the Saskatoon Ka and Q-Band centers for a flat spectrum in antenna temperature.

^(b) For the Saskatoon Ka and Q-Band data, $\hat{\alpha}$ has no units since these templates have units μK . For the DIRBE template, $\hat{\alpha}$ has units $\mu\text{K} (\text{MJy}/\text{sr})^{-1}$ since this template has units MJy/sr . For the 408 MHz and 1420 MHz surveys, $\hat{\alpha}$ has units $\mu\text{K} \text{K}^{-1}$ since these templates have units K .

^(c) The probability that a Gaussian random variable with mean zero and standard deviation $\sigma_{\hat{\alpha}}$ does not exceed $\hat{\alpha}$.

^(d) The Saskatoon Ka and Q-Band data, as well as the point source template, have units μK , the DIRBE far-infrared data has units MJy/sr , and the two synchrotron templates have units K .

^(e) The correlation between the Saskatoon data and the different templates is given as fluctuation percentage, defined as $\left(\frac{\hat{\alpha}}{\sigma_{SK}}\right) \sigma_{Gal}$, where $\sigma_{SK}=90.9 \mu\text{K}$ is the *rms* CMB fluctuations at 1° .

Table 2: Correlations with the Saskatoon (SK) Q-Band (40 GHz)^(a)

Template	$\hat{\alpha} \pm \sigma_{\hat{\alpha}}^{(b)}$	$\frac{\hat{\alpha}}{\sigma_{\hat{\alpha}}}$	Significance ^(c) (%)	$\sigma_{Gal}^{(d)}$	$\Delta T \equiv \hat{\alpha} \sigma_{Gal}$ (μK)	$\frac{\Delta T}{\sigma_{SK}}^{(e)}$ (%)
SK (Q-Band)	1.00±0.02	48.3	100	90.9	90.9±1.9	100
DIRBE 100 μm	15.0±8.1	1.9	97	1.30	19.5±10.5	21
Point Sources	0.2±3.5	0.1	52	0.50	0.1±1.7	0.1
408 MHz survey	−4.6±6.8			1.34	−6.1±9.1	−7
1420 MHz survey	−0.1±0.2			0.03	−0.00±0.01	−0.003

Table 3: Free-Free observations scaled to 40 GHz

References	Angular Resolution	Patch Size	ΔT (μK)
Fomalont et al. 1993	1 ′	7 ′×7 ′	<2.4
Gaustad et al. 1996	0.1°	7 °×7 °	<2.2
Reynolds et al. 1992	0.8°	12 °×10 °	2.6
Simonetti et al. 1996	1 °	7.5°×7.5°	<2.1
This work ^(a)	1 °	7.5°×7.5°	17.5± 9.5
K96a	10 °	b >30°	10.0± 3.9
K96b	10 °	b >30°	15.3± 3.6

^(a) Assuming dust emission with $\beta=2$, about 10% of the observed correlation between Saskatoon Q-Band data and DIRBE 100 μm template is due to dust and 90% is due to free-free emission. Adjusting the value (19.5±10.5) μK to (17.5±9.5) μK , we account for the residual dust contribution.

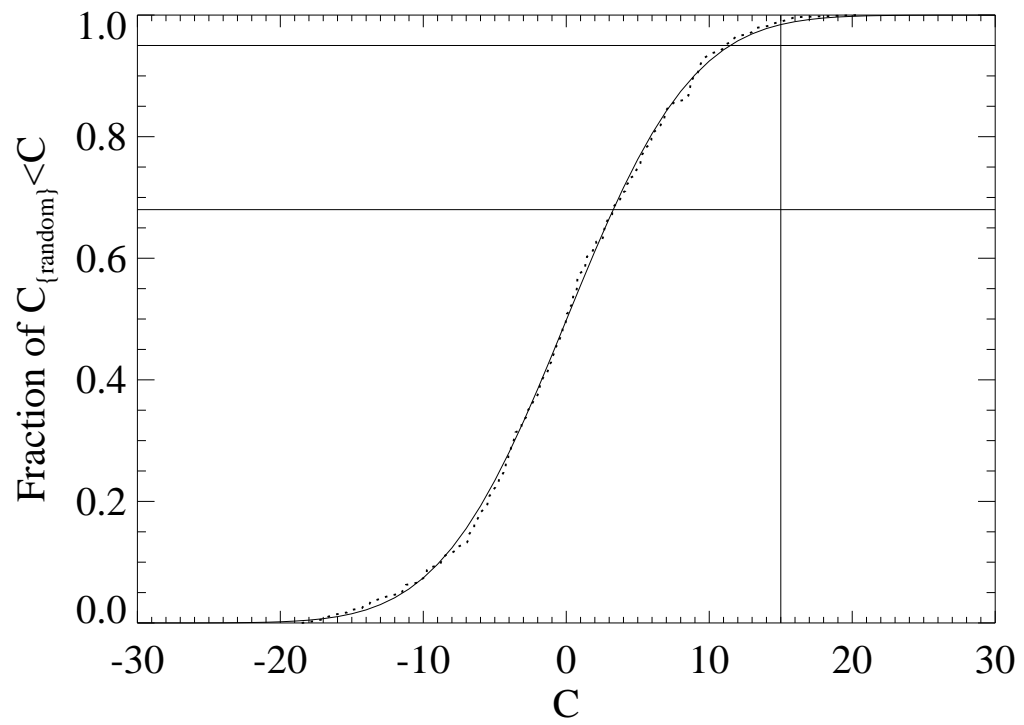
REFERENCES

- Bennett, C.L., Smoot, G.F., Hinshaw, et al. 1992, *ApJ*, 396, L7
- Bennett, C.L., Banday, A.J., Gorski, K.M., et al. 1996, *ApJ*, 464, L1
- Boguess, N.W., Mather, J.C., Weiss, et al. 1992, *ApJ*, 397, 420
- Brandt, W.N., Lawrence, C.R., Readhead, A.C.S., et al. 1994, *ApJ*, 424, 1
- Fomalont, E.B., Partridge, R.B., Lowenthal, J.D., et al. 1993, *AJ*, 404, 8
- Gaustad, J.E., McCullough, P.R., and Van Buren, D. 1996, *PASP* 108, 351
- Haslam, C.G.T., Klein, U., Salter, C.J., et al. 1981, *A&A*, 100, 209
- Kogut, A., Banday, A.J., Bennett, C.L., et al. 1996a, *ApJ*, 460, 1 (K96a)
- Kogut, A., Banday, A.J., Bennett, C.L., et al. 1996b, *ApJ*, 464, L5 (K96b)
- Kühr, H., Witzel, A., Pauliny-Toth, I.I.K., et al. 1981, *A&AS*, 45, 367
- Netterfield, C.B., Devlin, M.J., Jarosik, N., et al. 1997, *ApJ*, 474, 47 (N97)
- Partridge, R.B. 1995, *3K:The CMBR* (GB: Cambridge University)
- Reich, P., Reich, W. 1988, *A&AS*, 74, 7
- Reynolds, R.J. 1992, *ApJ*, 392, L35
- Simonetti, J.H., Dennison, B., Topasna, G.A. 1996, *ApJ*, 458, L1
- Tegmark, M., Efstathiou, G. 1996, *MNRAS*, 281, 1297
- Tegmark, M., de Oliveira-Costa, A., Devlin, M.J., et al. 1997, *ApJ*, 474, L77
(T97)
- Wollack, E.J., Devlin, M.J., Jarosik, N., et al. 1997, *ApJ*, 476, 440 (W97)

FIGURE CAPTIONS:

Fig. 1.— Saskatoon and template maps. For all maps, the temperatures are shown in coordinates where the North Celestial Pole is at the center of a circle of 15° diameter, with RA=0 at the top and increasing clockwise. From left to right, the three top panels show the Saskatoon Ka-Band map (Ka), the Saskatoon Q-Band map (Q) and the full Saskatoon (Ka+Q Bands) map (All). The three middle panels show the 408 MHz Haslam survey (Has), 1420 MHz Reich & Reich survey (RR) and the point source template (PS). Finally, the three bottom panels show the DIRBE 240, 140 and $100 \mu\text{m}$ maps.

Fig. 2.— Cumulative probability distribution for the correlation between DIRBE $100 \mu\text{m}$ and Saskatoon Q-Band data. The solid curve is for the case where $\hat{\alpha}$ is Gaussian with zero mean and variance given by equation (5). The dotted curve is for the 288 different DIRBE sky patches. The horizontal lines indicate the confidence levels of 68% and 95%, while the vertical line at $\hat{\alpha}=15.0$ represents the correlation value given by DIRBE template at the Saskatoon observing region.



de Oliveira-Costa, Kogut, Devlin, Netterfield, Page & Wollack (1997)

